Reference: *Biol. Bull.* **182:** 195–209. (April, 1992)

Architectural and Mechanical Properties of the Black Coral Skeleton (Coelenterata: Antipatharia): A Comparison of Two Species

KIHO KIM*, WALTER M. GOLDBERG**, AND GEORGE T. TAYLOR

Florida International University, Department of Biological Sciences, University Park, Miami, Florida 33199

Abstract. Black coral skeletons are laminated composites, composed primarily of chitin fibrils and non-fibrillar protein. This paper examines mechanical properties of the composite and the architecture of the chitin component. Two species are shown to differ significantly in their tensile strength and fibril structure. The skeleton of *Antipathes salix*, a Caribbean species of commercial value, is stiffer, harder, darker, more dense, and more hydrophobic than *Antipathes fiordensis* from New Zealand. The chitin fibrils constitute a greater proportion of the skeleton in *A. salix*, where they are helically wound in an anticlockwise pattern within layer. Adjacent layers of skeleton are arranged with relatively small layer-to-layer fibril biases. There is no evidence of "helicoidal" structure in this skeleton. The fibrils in *A. fiordensis* are also wound anticlockwise within layer, but with rather large fibril biases between layers, giving the appearance of a meshwork. Large-scale helicoidal patterns with apparent rotations of 180° characterize this material. Skeletal architecture is compared with the cuticle of insects and other arthropods. The skeletons of both species exhibit spines characteristic of the Antipatharia. We suggest that these have a significant reinforcing effect on the strength of the skeleton, contributing to an overdesign for the habitat in which these organisms presently occur.

Introduction

Black corals are well known as articles of commerce in the jewelry and curio trade dating from at least the time of the ancient Greeks (Hickson, 1924). The skeleton can be polished to an onyx-like luster, but because it is organic, it can also be bent and molded while being heated. Consequently, this material is highly prized in the jewelry trade, and collection pressure has resulted in the listing of black corals in the Convention for the International Trade in Endangered Species (CITES) (Wood and Wells, 1988). Collection pressure notwithstanding, certain species of black coral may constitute a substantial part of the fauna on deep reefs and in other more geographically restricted habitats. In the Fiordland district on the southwest coast of New Zealand's south island, for example, the endemic black coral, *Antipathes fiordensis* Grange is the dominant macrobenthic organism in depths of 10–20 m (Grange, 1985, 1990). Similarly, *Antipathes salix* Pourtalès, is one of the more commonly occurring black coral species in the Caribbean, although it is most often restricted to coral reef slopes below 30–40 m. Yet in spite of their commoness in some areas, rarity or endangerment in others, and their historical and commercial value, black corals remain among the least known of colonial coelenterates. Almost nothing is known about the architectural and material properties of black coral skeleton, which may determine not only its commercial value, but its ecological functions as well. This paper is the first attempt to elucidate and compare the structural and mechanical properties of black coral skeleton, using as examples the geographically disparate congeners *A. fiordensis* and *A. salix*.

Materials and Methods

Colonies of *A. fiordensis* were collected by SCUBA divers at Doubtful Sound, New Zealand, in 10–20 m depth, and *A. salix* at Cay Sal Bank, Bahamas, in 30–40 m. Liv-

Received 21 October 1991; accepted 24 January 1992.

* Current address: State University of New York at Buffalo, Department of Biological Sciences, Buffalo, New York, 14260.

** To whom correspondence should be addressed.

ing tissue was removed by jets of fresh water, and the remaining skeletal material was stored dry at 4°C.

Microscopy

Skeletal material was examined both before and after treatment with a variety of agents. Some skeleton was examined after standard double fixation (3% glutaraldehyde and 1% osmium tetroxide) and double staining (saturated uranyl acetate in 50% methanol and 0.3% lead citrate). However, because the fibrils comprising the skeleton of both species are embedded in an amorphous, resistant matrix, observation of fibrillar orientation or structure often required chemical treatment. Unfixed material was placed in concentrated formic acid for 24–48 h at room temperature to cause swelling and delamination of the skeletal layers (Goldberg, 1991). Using watchmaker's forceps, narrow strips of the outer skeleton were torn away along the long axis. Formic acid-treated material was washed and dehydrated in graded ethanols and embedded in Spurr resin. Thin sections were taken at parallel, 45° and perpendicular to the long axis of the branch. Additional material was examined after deproteination with 1 *N* KOH (24 h, 105°C; Hackman and Goldberg, 1971). Sections were stained with 2% phosphotungstic acid (PTA) in 10% ethanol (Bouligand, 1972) and examined using a Phillips EM 300 transmission electron microscope (TEM) operated at 60 kV. Fine structural observations of fibril orientation by scanning electron microscopy (SEM) could not be made without etching the smooth surface of formic acid-treated material with 1.0 M $NaBH_4$ in 1.0 M NaOH (4 h, 70°C). The delaminated, etched skeleton was dried after ethanol dehydration and coated with Au/Pd prior to examination in an ISI Super 3A SEM. We also prepared fracture cross-sections for SEM from acid-treated material. Samples of untreated, as well as formic acid-treated, and KOH-treated skeleton were examined in the light microscope. One micron sections of Spurr-embedded material were either stained with Toluidine blue, or viewed unstained using polarized light and/or phase-contrast microscopy. We also examined unembedded, aqueous mounts, and epoxy-embedded thick sections ground and polished with graded abrasives.

Material properties

Measurements of density and Young's modulus were performed on skeleton rehydrated in artificial seawater (ASW). To estimate minimum time required for rehydration, skeletal pieces of various diameters and lengths were dried overnight at 70°C, and cooled in a desiccator. The dry skeletons were weighed, placed in ASW (~37‰, room temperature), then surface-dried and re-weighed daily. When weights for three consecutive days were within 0.5%, hydration was considered complete and the gravimetric change was noted as the water content. The rehydrated piece was surface-dried and placed in a graduated cylinder (accurate to 0.01 ml). Density was calculated as weight of the skeleton divided by the volume of water displaced.

Mechanical properties were determined using samples 6–10 cm long and 0.7–1.5 mm in diameter, embedded in methyl methacrylate at both ends prior to rehydration. We were limited to branches less than 1.5 mm in diameter because larger branches pulled out of the plastic before failing. The plastic ends were loaded under tension using an Instron 1011 strength tester fitted with a 5 kg cross head travelling at a constant rate of 50 mm/min. The Young's modulus (E) was calculated using the formula, $E = FL/AdL$, where F and dL are the amount of force applied to the branch and the change in its length at failure, respectively. The length of the skeleton (L) is the distance between the two methyl methacrylate blocks, while A is the cross sectional area of the sample. Because the skeleton was never perfectly cylindrical and often tapered toward the apex, an average cross sectional area was estimated by assuming the taper was linear from one end to the other. Hardness was measured on both the Moh's and Vicker's scale. Moh's is a qualitative scale in which 10 minerals are used as standards ranging from talc (1) to diamond (10). Hardness is based on the ability of one material to scratch another. The Vicker's scale is a more quantitative measure of microhardness, which measures the impression made using a pyramid-shaped diamond forced into the surface of a material. Microhardness is expressed as Vickers Hardness Numbers according to the formula $VHN = 1854P/d^2$ (kg mm^{-2}), where P is the load in grams and d is the mean length of the indentation in microns (*cf.*, Hillerton *et al.*, 1982). Testing was performed both parallel and perpendicular to the long axis of hydrated and unhydrated skeleton using a Leco-DM 400F hardness tester with an applied load of 10 g.

Skeletal chemistry

Protein content and amino acid composition were determined after hydrolysis in 4 *N* methanesulfonic acid (105°C, 20 h) (Simpson *et al.*, 1976) using a JEOL 5AH amino acid analyzer with a ninhydrin-based detection system. Protein was expressed as total ninhydrin reactivity. Chitin was estimated from the amino sugar content, corrected for deacetylation. Dry skeletal powder was extracted using chloroform:methanol (2:1, V:V) on a shaker for 48 h at room temperature. The powder was washed in methanol (3×), dried overnight, and re-weighed to estimate lipid content.

Results

Microscopy

The external surfaces of antipatharian skeletons are distinguished by the presence of spines. Both the spine morphology and pattern of spination clearly distinguish the two species, and correspond with skeletal characters given by Grange (1988, 1990) and Opresko (1972). The skeleton of *A. fiordensis* is marked by rows of numerous, smooth, slender spines 200–350 μm long in addition to shorter, branched secondaries (Fig. 1). In contrast, spines in *A. salix* are relatively uniform, compressed cones 90–100 μm long, that become nodose during maturation (Fig. 5, inset). As is typical of antipatharians (Opresko, 1972), the spines are organized into spiralling rows along the long axis of the skeleton (Fig. 5). There are no secondary spines in this species.

In light microscopic cross sections of *A. fiordensis*, the growing tip can be distinguished clearly from more mature portions of the skeleton, as a region that stains intensely with Toluidine blue (Fig. 9). The skeleton increases in thickness and in length by adding thin *growth layers* or *lamellae*. These range in thickness from 0.1 to 1.0 μm when measured between the spines (Fig. 14). The lamellae become thinner as they approach and add a layer to the spines. Most of the layers are separated from each other by a subtle discontinuity in optical density. However, at irregular intervals, material that stains more intensely with Toluidine blue separates sets of skeletal lamellae. These deposits, which are also osmiophilic, are visually interpreted as *growth rings*. Growth ring structure has been described by Goldberg (1991). Ring timing in this species will be considered elsewhere (Grange and Goldberg, in prep.).

Strongly birefringent patterns are observed when thin pieces of formic acid-treated skeleton are examined with polarized light microscopy. These patterns appear to result from the chitin fibrils because subsequent deproteination by KOH, albeit incomplete (see skeletal chemistry section below), does not appreciably affect the birefringence of either species. Light microscopic observation of *A. fiordensis* skeleton suggests that the fibrils form anticlockwise helices around the long axis of the branch. Interpretation of the longitudinal pattern is influenced by the presence of numerous spines that serve as convergence points for the fibrils within layers. The spines are numerous enough to obscure the surface fibril pattern, making an accurate assessment of its overall direction difficult. A view through several lamellae creates the appearance of a meshwork (Fig. 10), indicating a layer-to-layer change in the fibrillar winding pattern.

Visualization of *A. fiordensis* chitin microfibrils (hereafter referred to simply as fibrils) by transmission electron microscopy requires treatment with formic acid, or formic acid followed by KOH. In transverse section, the fibrils constituting a lamella appear to be sub-parallel and woven. At intervals, the fibrils are sparse, and it is here that the lamellae separate with KOH or formic acid (Fig. 14, inset). Although chemical treatment removes the electron-opaque material that defines a lamella, it is clear that there are several sublayers of fibrils within each of them. Sections of formic acid-treated material cut at 45° to the skeletal long axis show tracts of fibrils within several adjacent lamellae. Most of the tracts appear to intersect at angles, giving them a twisted or cable-like appearance (Fig. 15). This pattern may be expected from helically wound fibrils in successive layers that are out of phase. There are no lamellae that clearly display fibrils with a preferred orientation, and there are no differences in fibril pattern when material is sectioned transversely. There are irregularly spaced regions of skeleton displaying parabolic or arced patterns, suggesting a systematic, gradual rotation of fibrils among adjacent lamellae (Fig. 15 and inset). However, these are not as obvious in the electron microscope as they are in the light microscope (see below).

Longitudinal preparations indicate that fibrils intersect and overlap one another, displaying gradual changes in orientation (Fig. 16). In some of our preparations there are abrupt changes in orientation particularly in the spines, where fibrils within layer are perpendicular to the long axis. In addition, we note again that each lamella is composed of multiple sublayers with different orientations. Because some of these sublayers may only be 10 nm thick (Figs. 14, inset; 15), thin sections of 90 nm may cut through more than one set of fibrils. Thus the TEM pattern that appears to show intersecting fibrils, may be an artefact. In the SEM, the surface pattern of fibrils within layer is clearer (Fig. 2). Spines are responsible for the large changes in orientation at the top and bottom of the figure. Figure 2 is a surface view of the multiple layers shown in Figure 10. Fibrils appear to fan out between spines but actually wind helically in the longer run.

If the etched surfaces of adjacent layers are examined using SEM, large fibrillar biases (*i.e.*, large angular deviations) can be seen resulting from layer to layer changes in fibril direction. In Figure 4, for example, 30 to 40° changes occur in adjacent lamellae. Up to 45° changes occur between layers in this species. The fracture pattern also suggests a change in fibril orientation, resulting in layers that fracture in different directions (Fig. 3). Perhaps the most revealing view of this complexly arranged skeleton is the ground thick section shown in Figure 11. This transverse section shows that the skeleton is organized into large-scale patterns that are difficult to see at the electron microscopic level. The cable-like arrangements of fibrils appear to be a limited, thin-sectional view of mul-


1

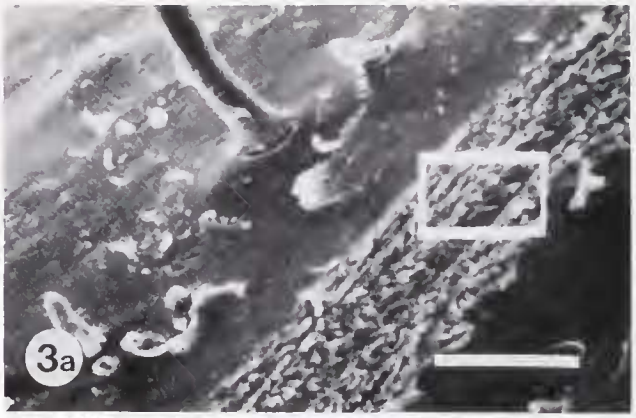
3a


3b

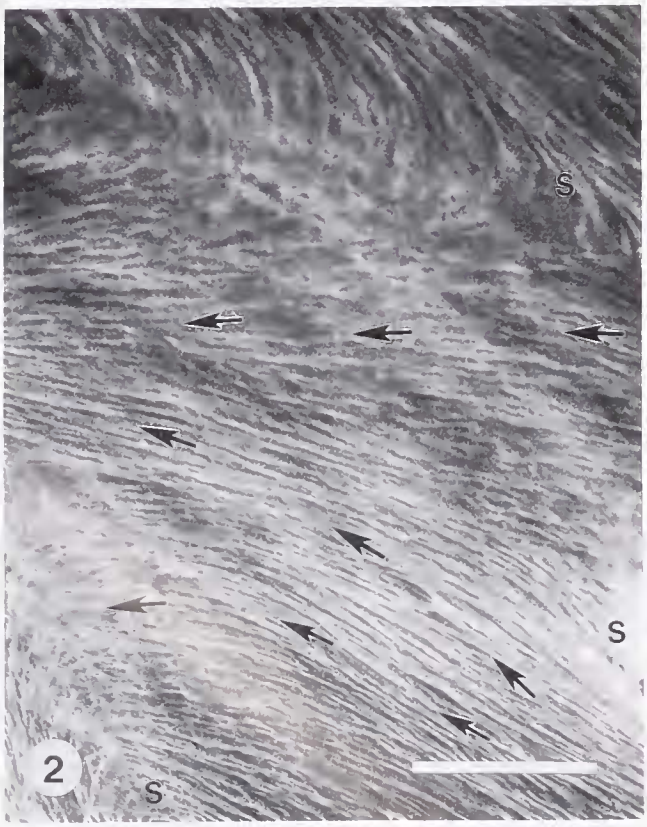
S
S
S
2


4

tiple layers, each of which has small deviations in fibril orientation. Constructive superimposition of fibrillar tracts with similar orientation (but not parallel), give rise to darker tracts of fibrils in polarized light. Regions between tracts give rise to lighter, diffuse areas, representing regions of abrupt change in fibril orientation in successive layers of skeleton. Thus, large (10–20 μ), irregularly spaced helicoids are formed that appear to rotate through 180° (Fig. 15).

Light microscopic cross sections of *A. salix* skeleton are striking in their apparent uniformity compared to *A. fiordensis*. This appearance is due to several factors. First, there are no ontogenetic differences in the staining properties of the skeleton. Instead, clusters of lamellae alternately stain ortho- and metachromatically with Toluidine blue (Fig. 12). Second, the skeleton lacks the irregular deposits of osmiophilic material seen as growth rings in the New Zealand species (compare Figs. 12 and 9). Growth rings in *A. salix* are very subtle and appear in unstained material as slight but regular differences in spacing between clusters of lamellae. This subtle structural distinction all but disappears on staining with Toluidine blue. Electron microscope observations suggest that rings correspond to a particular arrangement of fibrils (see below). This is a structural distinction in the formation of growth rings in the two species. In *A. fiordensis*, rings are osmiophilic and non-fibrillar (Goldberg, 1991). Polarized light examination of KOH treated *A. salix* branches suggest that the fibrils are wound around the long axis of the skeleton following the gradual, left handed spiral pattern of the spines. Fibrillar tracts between spines tend to be more densely packed than they are around and within the spines themselves (Fig. 13) in contrast to *A. fiordensis*. Fibrils in successive layers reinforce this pattern resulting in alternately opaque and translucent zones of birefringence parallel to the skeletal axis. This pattern suggests the absence of large fibril biases as in *A. fiordensis*.

Transverse sections of *A. salix* skeleton (TEM) are organized into a series of light and dark bands that vary in their specific characteristics, and range in thickness from 0.1 to 1.9 μm. Individual lamellae appear to correspond to these bands. The darkest regions consist of densely packed fibrils arranged in parallel within a matrix with a strong affinity for PTA. These grade into bands of intermediate electron opacity that constitute the largest volume of skeletal cross section. The intermediate bands may contain fibrils in a number of planes, including parallel. The lightest bands appear to be narrow (0.1–0.2 μm) regions where fibrils are obliquely arranged (Fig. 17). Although it is difficult to determine with certainty, growth rings appear to correspond to the juxtaposition of light and dark bands within a series of lamellae (Fig. 18). Fibrils in longitudinal sections occur in bands that remain parallel for relatively long distances, and vary in their electron opacity (Fig. 19). This structure corresponds to a section through a band of intermediate electron opacity as seen in cross section (*e.g.*, upper part of Fig. 18), where fibrils occur with minor variations in orientation.

Fracture preparations more clearly show the parallel structure of the lamellae in *A. salix* (Fig. 6). These result from the smaller fibril biases between lamellae in this species (compare with Fig. 3). In SEM preparations the surface fibrils appear to be arranged in a chevron-like pattern (Fig. 7). However, our overall view of the surface fibril pattern in this species is limited due to its less tractable response to chemical and physical manipulation. While formic acid separates the skeleton into layers (Fig. 6, inset), individual lamellae do not separate well, even with mechanical assistance. Additionally, because of the relative uniformity of fibril distribution, phase contrast and polarized light microscopy is not useful in determining the fibril pattern over long distances. Scanning electron microscopy is more successful in showing between-layer changes in fibril orientation over short distances, although etching with borohydride is not as effective in revealing surface fibril patterns in this species. Changes in fibril orientation do occur between layers, however, the fibril biases are small (<20°) compared to *A. fiordensis* (compare Figs. 4 and 8).

Material properties

The Young's modulus is a measure of stiffness or rigidity derived from a simple elastic behavior of materials

Figures 1–4. SEM preparations of *Antipathes fiordensis*.

Figure 1. Branch surface and its numerous and prominent spines; scale bar = 500 μm.

Figure 2. Borohydride-etched branch surface showing complex pattern resulting from counterclockwise winding of surface fibrils (arrows) around numerous spines (s), and the three-dimensional pattern of fibrils in spines themselves. The spine at the top of the figure depicts the change in orientation of fibrils at its base; scale bar = 10 μm.

Figure 3. Fracture pattern of formic acid-treated skeleton. 3b (scale bar = 5 μm) corresponds to the boxed area in 3a (scale bar = 50 μm). Large fibril biases between layers result in lamellae that fracture in different directions; arrows depict fibril orientation within the indicated layer.

Figure 4. Fibril biases of up to 45° (arrows) are encountered when comparing surface fibrils of successive lamellae (formic acid-borohydride preparation); scale bar = 10 μm.


5


7

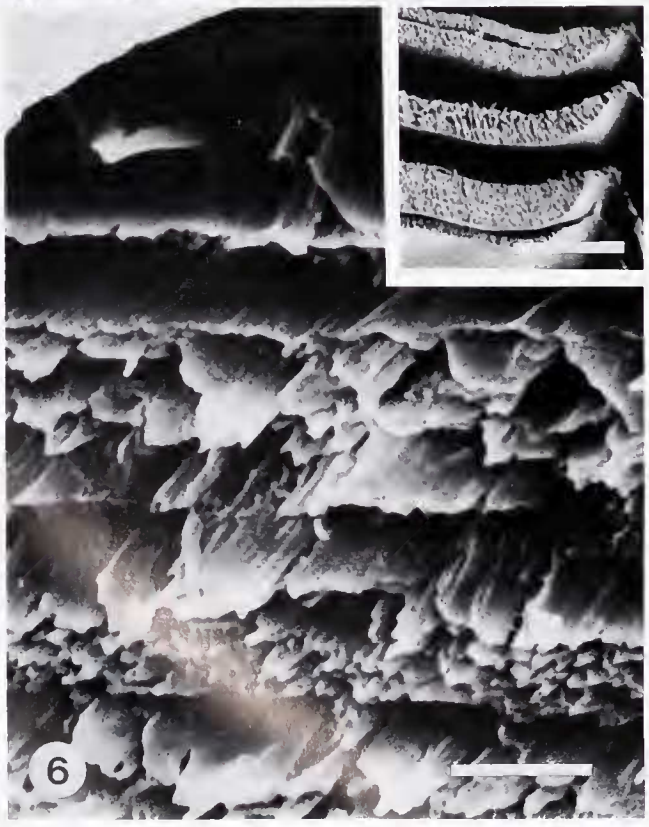
6


8

in which stress is proportional to strain, although this proportionality rarely occurs in most materials of biological origin (Hepburn and Chandler, 1980). We calculated Young's modulus from the sigmoidal load-deformation curve of the antipatharian skeleton (*e.g.*, Fig. 20). A small initial lag occurs as the specimen straightens under tension. This is followed by a linear region typically constituting >80% of the distance between the points of origin and failure. The terminal plastic region, where the greatest amount of deformation occurs just before failure, typically constitutes less than 12% of the stress-strain relationship. There is little deviation in the slope of the plastic region, and failure almost always occurs at the test grips. Moduli were calculated using only the linear portion of the curve, and again, using the slope of a line drawn between the origin and the point of failure. Only minor differences were noted. However, we also found that using only the linear portion was more prone to operator error. The moduli reported here were determined by the second method, which gives the average slope of the entire stress-strain relationship. This method is therefore more conservative compared to those determined solely from the slope of the more limited, linear portions of the load-deformation curve (see Bassin *et al.*, 1979; Vincent and Hillerton, 1979).

The material properties of the two antipatharians are very different (Table I, Fig. 21). In addition to being stiffer (more rigid), the skeleton of *A. salix* is more resistant to deformation under tension than *A. fiordensis* ($P < 0.0001$, for both cases). Higher density (12%) is also characteristic of *A. salix*, as is greater hardness. Hardness is a complex measure of material strength and plasticity. Although there are no absolute standards for hardness, a comparative measurement adds an additional perspective for this little-known material. The differences in skeletal hardness are not resolved on the Moh's scale because both skeletons, wet or dry, have hardnesses of 3, *i.e.*, both skeletons are only hard enough to scratch calcite. However, calcite is more readily scratched using *A. salix*, indicating that it is slightly harder than *A. fiordensis*. Microhardness testing further refines this observation, suggesting that *A. salix* is approximately 17% harder and less variable along both axes of testing compared to *A. fiordensis* (Table I).

Skeletal chemistry

We used amino acid analysis to estimate the relative proportions of skeletal chitin and protein. Standard methods of colorimetric analysis (*e.g.*, Lowry or Bradford) consistently underestimate protein levels. Chitin can not be estimated gravimetrically after "deproteination" with KOH because a variable amount of protein remains associated with the chitin after treatment. Table II summarizes these results. The skeletal tips are composed primarily of protein and chitin. Extractable lipid is both low and variable in the two species. The percent protein is greater in *A. fiordensis* ($P < 0.025$) and, conversely, there is a greater proportion of chitin in *A. salix* ($P < 0.05$). Overall, there are few differences in the amino acid composition of the skeletons (data not shown). When sequentially treated with formic acid and aqueous borohydride, some 6 to 9% of the protein is lost (Table III). Although there are some differences in protein composition resulting from this chemical treatment, the most significant change is the total destruction of tryptophan. The dominant amino acids, glycine, alanine, and histidine, are unaffected, as are the levels of glucosamine (*i.e.*, chitin). The principal effect of this reagent is the visual enhancement of chitin fibrils in the scanning electron microscope (see below).

Discussion

There are a number of commonalities between arthropod cuticle and antipatharian skeleton. Some of the general similarities in chemical composition have been described recently (Holl *et al.*, 1992). Arthropod cuticle also provides the basis of morphological comparison or contrast, because it is the most commonly studied example of chitin-protein architecture. Like antipatharian skeleton, cuticle is a composite material constructed of chitin fibrils embedded in an amorphous protein matrix. Cuticle is generally considered as a laminated structure with chitin fibrils lying in parallel within each layer. Layer-to-layer changes in fibril orientation have been characterized, ranging from the rare, totally uniform fibril orientation, to a helicoidal arrangement. Helicoids, as originally described by Bouligand (1965), are optical artefacts of arced

Figures 5–8. SEM preparations of *Antipathes salix*.

Figure 5. Branch surface showing spiral pattern of spines; scale bar = 200 μm. Inset: spines are laterally compressed and nodose; scale bar = 50 μm.

Figure 6. Fracture pattern showing parallel orientations of adjacent lamellae; scale bar = 5 μm. Inset: formic acid treatment does not separate adjacent lamellae, but separates the skeleton into thicker layers, possibly corresponding to growth rings; scale bar = 50 μm.

Figure 7. Surface fibrils, revealed by borohydride-formic acid treatment, are more unidirectional compared to *A. fiordensis*, and form convergent, chevron-like tracts; scale bar = 10 μm.

Figure 8. Adjacent lamellae display relatively small fibril biases; mean direction is depicted by arrows; treatment as in Figure 7; scale bar = 10 μm.

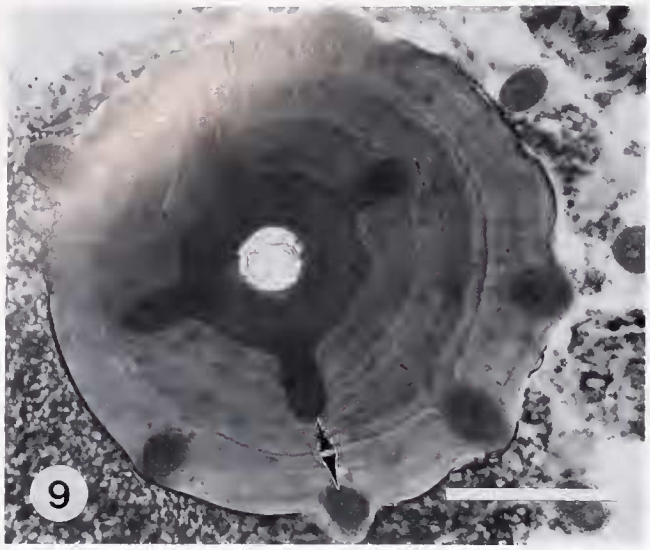
9

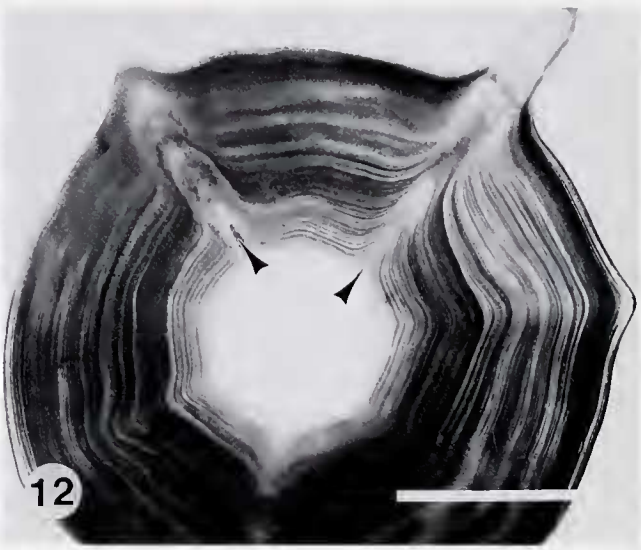
12

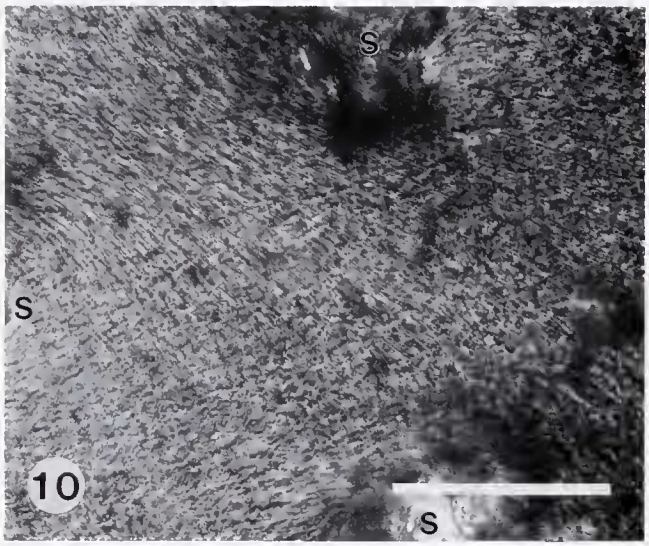
S
S
S
10

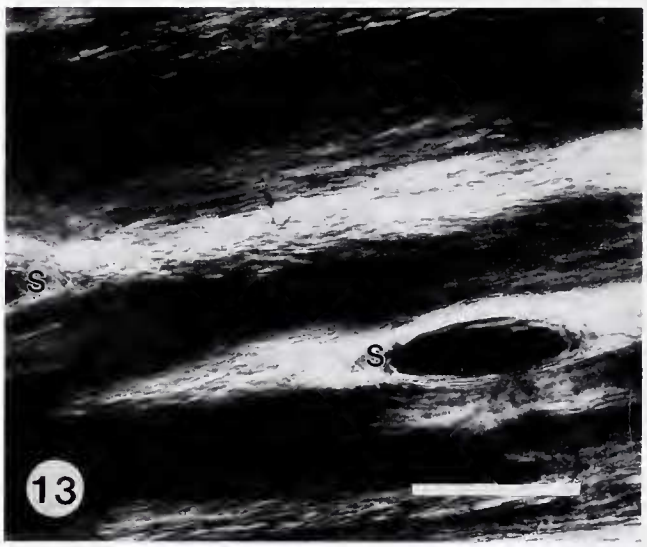
S
S
13


11

or parabolic fibril patterns when multiple layers of parallel fibrils are viewed obliquely or transversely. Helicoids are formed by adjacent fibril layers that appear to rotate gradually from parallel. There are several variations on this theme. Growth layers, consisting of parallel chitin fibrils formed during the day, alternate with helicoidal layers deposited at night in some insect groups (Neville and Luke, 1969). A "plywood" type of architecture can be formed by some insects when parallel layers abruptly change direction on each successive day by about 90°. Alternatively, a pseudo-orthogonal "plywood" cuticle can be formed by more gradual changes in orientation of daily parallel fibril layers. In the latter case, helicoidal layers may rotate gradually through 90° or 180° before a daily parallel layer is deposited. Finally, some insects may not deposit a daily parallel layer of chitin fibrils at all, thus producing the appearance of continuous rotation (Neville, 1967, 1970; Barth, 1973). The helicoidal model is the most common explanation of cuticular structure, especially among insects (*cf.*, Filshie, 1982; Neville, 1984; Hughes, 1987) and crustaceans (*cf.*, Bouligand, 1971; Giraud-Guille, 1984; Compere and Goffinet, 1987). Chitin helicoids have also been described from a whelk periostracum (Hunt and Oates, 1984) and the test of a tunicate (Gubb, 1975). While the helicoidal model has gained wide acceptance, agreement is not universal. Important exceptions to the parallel fibril model include the presence of vertical fibrils supporting the horizontal lamellae in some arthropods (*cf.*, Hepburn and Chandler, 1976). Others have more generally disputed the helicoidal model, suggesting that the layers of fibrils are indeed curved and are not artefactual (Dennell, 1973; Dalingwater, 1975). Helically wound and crossed chitin fibrils occur in certain insect groups but scant attention is paid to them in the modern literature.

Both antipatharian skeletons are composed of helically wound fibrils. They are unlike the crossed fibrillar chitin described from insects, which form alternating layers of left and right handed helices (Neville, 1967). Figure 22 is a composite model of fibril structure, based on our microscopic observations. *Antipathes salix* skeleton is a comparatively simple structure composed of layers with small deviations in fibril orientation. Regions of parallel fibril and sub-parallel orientation are common. Regions of abrupt change in fibril orientation may constitute optical discontinuities that appear as growth rings, but helicoidally arranged layers as such, are absent. *Antipathes fiordensis* skeleton is much more complex. Fibrils within layer exhibit a more "active" pattern. There is a considerable degree of angular change from one layer to the next, as shown in both transverse and longitudinal sections. The helicoidal arrangement of the skeleton cannot be depicted easily because the pattern is obscured by the helically wound fibrils, the pattern of spination, and the irregular thickness of skeletal layers. If these factors are taken into account, the skeleton corresponds most closely to a type D insect cuticle (Barth, 1973) characterized by a helicoidal rotation of approximately 180° between parallel (in this case low angle, cable-like) fibrils.

A helical arrangement of the fibrils provides some flexibility while preventing explosion and localized buckling under multiaxial stress (Wainwright *et al.*, 1976). However, in many helically wound structures there is a danger of delamination caused by the incompatibility of strain

Figures 9–11. Light microscope preparations of *Antipathes fiordensis*.

Figure 9. Transverse 1-μm thick section showing intensely stained (Toluidine blue) young skeleton, followed by lightly stained region marked by irregular, dark growth rings. Spines at the periphery (arrowheads) are obliquely sectioned; scale bar = 100 μm.

Figure 10. Formic acid-treated skeletal peel (unstained) examined with a combination of polarizing and phase contrast optics shows the intersecting pattern of fibrils from several skeletal layers. Surface fibrils converge around the bases of the spines (s); the long axis of the skeleton is parallel to the scale bar. Scale = 50 μm.

Figure 11. Polished transverse section showing irregularly spaced, large scale helicoids. Cable-like fibrils with acute angles constitute the helicoid boundaries (straight arrows). Apparent rotation of successive fibril layers form the helix-like structures depicted by curved arrows. Fibrils converge with a longitudinally sectioned spine at the bottom of the figure; scale bar = 50 μm.

Figures 12–13. Light microscopic preparations of *Antipathes salix*.

Figure 12. Transverse 1-μm thick section showing differential orthochromatic (dark layers) and metachromatic (light layers) staining with Toluidine blue. The skeleton of this species is composed of multiple lamellae, but does not have distinct, differentially staining growth rings; the incremental growth of spines (arrowheads) is also shown; scale = 100 μm.

Figure 13. Formic acid-treated skeletal peel (unstained) examined with a combination of polarizing and phase contrast optics shows both convergent and parallel fibrils arranged in birefringent light and dark bands. In contrast to the New Zealand species, the fibrils tend to be more densely arranged between spines (s). This view through multiple lamellae suggests that large fibril biases are not a prominent feature of this species; the long axis of the skeleton is parallel to the scale bar; scale = 50 μm.

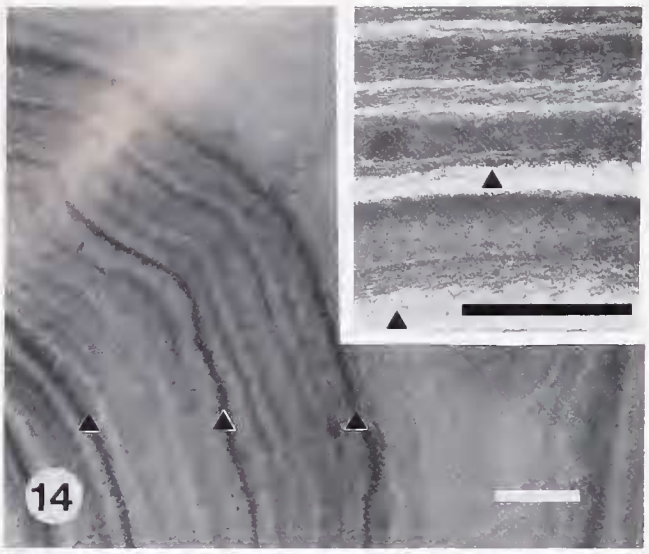
14

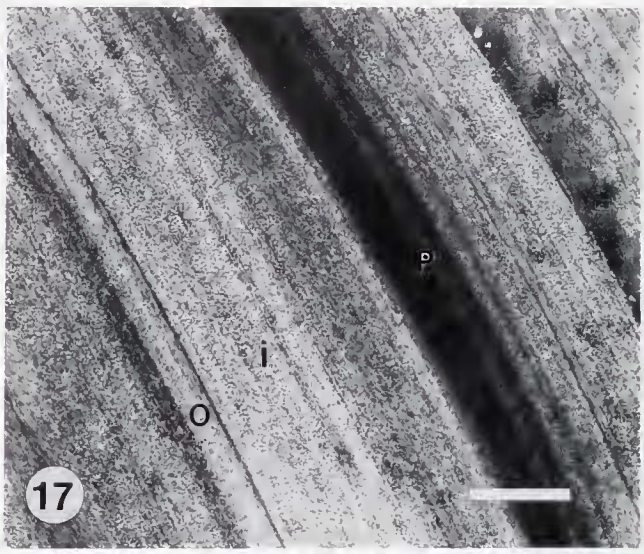
p
i
o
17

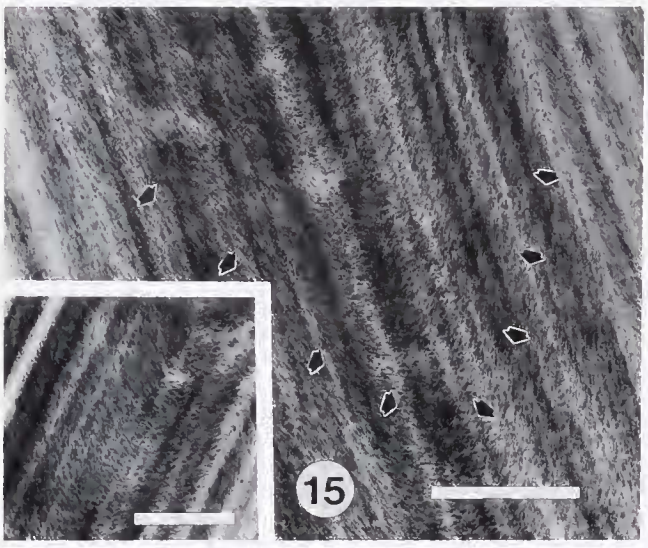
15

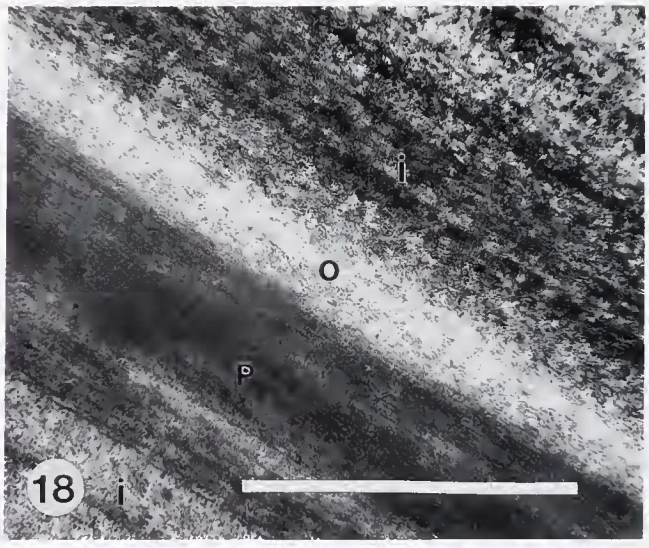
i
o
p
18
i


16

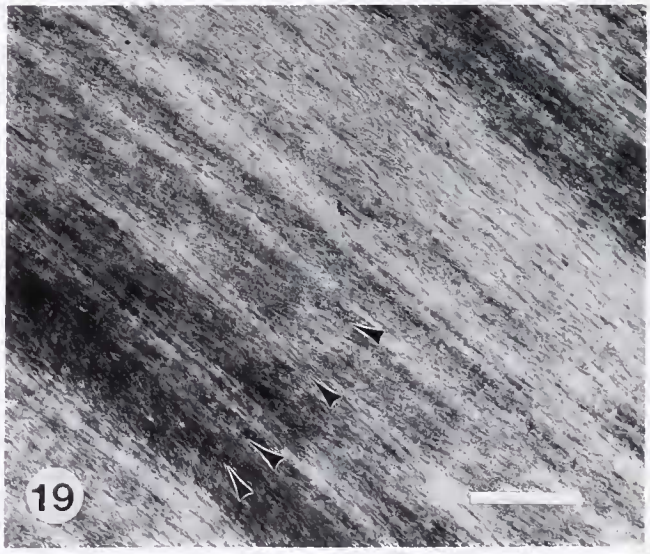
19

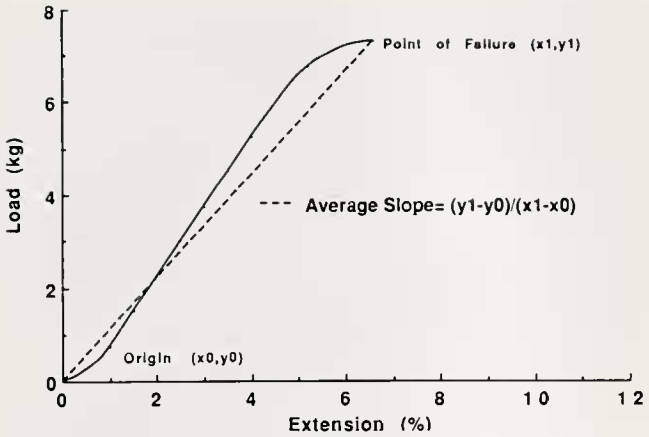

Figure 20. Typical load-deformation curve (solid line) from antipatharian skeleton depicting the method of calculating Young's modulus from the average slope (dashed line) of the stress-strain relationship. Extensibility is the percent elongation of the specimen at failure.

between adjacent layers with different fibril orientations (Wainwright *et al.*, 1976). One way of dealing with this is to allow only small angular differences between fibrils in adjacent layers as in certain types of helicoidally arranged insect cuticle. However, in antipatharian skeleton, the layers are not simple laminated structures. Because the spines are cemented and inserted layer upon layer, the helically wound skeleton is fixed at multiple points. We hypothesize that the spines increase the surface area for cementing one skeletal layer to the next. Moreover, they may play an important role as continuous rivets, preventing delamination from shear forces produced by skeletal bending and torsion. If this suggestion is correct, the presence of spines should reduce or eliminate the requirement of small fibril biases between helically wound layers.

In addition to differences in fiber patterns, there are a number of other disparities inherent in the diversity among the insect cuticles that make mechanical comparisons with black coral skeletons difficult. There are male-female differences, maturational differences, and regional differences within single cuticles. There are also differences in technique among investigators, some of whom have apparently performed mechanical testing without taking water content into account (see review by Vincent, 1980). The data given by Vincent show, not surprisingly, that stiffness values in insect cuticle vary from 1×10^6 Nm^{-2} to 17 GN m^{-2}, with a mean of 1.8 GN m^{-2} for all 28 cases. While the Young's modulus of the black corals studied here fall in line with the mean, the stiffest of insect cuticle can be as stiff as compact bone (see Hepburn and Joffe, 1976; Vincent and Hillerton, 1979). It is doubtful that antipatharian skeleton from a comparable number of species will be found with a comparable range of values.

In a composite structure, the fibrils can be expected to stiffen the more deformable matrix by reinforcing it. The degree of reinforcement should increase quickly with increasing volume to about 10–20%, irrespective of the fibril orientation, after which gains in stiffness become dispro-

---

Figures 14–16. Transmission electron microscope preparations of *Antipathes fiordensis*. Scale bars = 1.0 μm.

Figure 14. Transverse section of doubly fixed, doubly stained skeleton. Lamellae or growth layers are defined by weak osmiophilia or subtle changes in electron opacity (between triangles). Growth rings are perceived as darker or thicker regions of osmium deposition (triangles). Inset: treatment with formic acid and KOH removes protein matrix and osmiophilic material (triangles). Lamellae are composed of fibrils in a variety of orientations, and tend to separate where the fibrils may be diffuse or absent (transverse section).

Figure 15. Formic acid-treated, PTA-stained skeleton sectioned at 45°: skeletal layers consist of light and dark bands. The more prominent dark, cable-like fibrils are interpreted to result from the optical intersection of helically wound fibril layers; light regions are areas where fibrils appear to undergo rotation. Portions of larger scale helicoids, resulting from regular change in fibril bias in successive lamellae, can be seen by focusing on the overall pattern of apparent curvature (arrows). Inset: detail of a partial helicoid.

Figure 16. Formic acid-treated longitudinal section showing gradually intersecting (arrowheads) and abrupt changes in fibril orientation (curved arrow). The latter can be due to the presence of spines (compare with Fig. 2), or a section through more than one layer of fibrils; PTA stain.

Figures 17–19. Transmission electron microscope preparations of *Antipathes salix*. Scale bars = 1.0 μm.

Figure 17. Transverse section showing lamellae with differing fibrillar orientations and electron opacities. O = zone of obliquely oriented fibrils; P = region of parallel fibrils; and i = intermediate zone. Fibril orientations parallel to the long axis of the skeleton are prominent in this species.

Figure 18. Detail of cross section showing electron opaque lamella with parallel orientation followed by narrow, electron-lucent zone of obliquely oriented fibrils and zone of intermediate electron opacity with several changes in fibril orientation; symbols as above.

Figure 19. Longitudinal section showing parallel and sub-parallel orientation (arrowheads) of fibrillar tracts (compare with Fig. 7). All preparations doubly fixed; PTA stained.

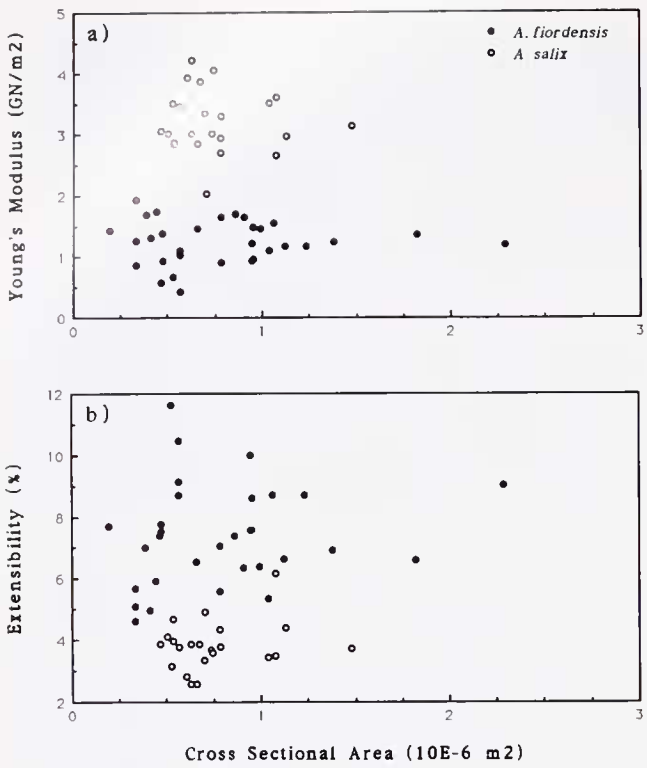

Figure 21. Scattergrams of (a) Young's modulus and (b) extensibility of the skeleton in *Antipathes fiordensis* and *A. salix* plotted against cross-sectional area. Young's modulus is determined from the average slope of the load-deformation curve (see text); extensibility is the percent elongation of the specimen at failure. The small degree of overlap in the data reflects significant differences in mechanical properties. Statistics are given in Table I.

portionately smaller (Wainwright *et al.*, 1976). Insect cuticle is highly variable in its chitin content, ranging from 4 to 60% (Vincent, 1980). In stiff cuticle, the chitin content tends to be 30 to 40% of the dry weight, while in more pliant cuticle, the chitin content tends to be higher, on the order of 50–60% of dry weight (Vincent, 1980; Hillerton, 1984). Black coral skeleton examined thus far contains a relatively low proportion of chitin, ranging from 6 to about 15% (Goldberg, 1978; this paper), and corresponds to published Young's modulus values for stiff cuticle. Although it is not yet possible to allocate mechanical properties to specific components of the skeleton, the greater chitin content of *A. salix* (~29% more than the mean of *A. fiordensis*) is within the overall range of chitin values where the difference may account for at least some of the increased skeletal stiffness.

The antipatharians are less rigid than a number of other biological materials, including wood, bone, mollusk shell, and some insect cuticle, while having a density higher than wood, lower than shell or bone, but about the same as insect cuticle (Wainwright *et al.*, 1976; Table 5.3). The ratio of Young's modulus to density (E/p) is the specific modulus, a means of assessing the stiffness per unit weight of materials. High values of specific stiffness are often considered superior to low values because they enable construction of stiffer and lighter structures. However, for antipatharians, greater flexibility per unit of density should be more important than stiffness. Thus antipatharians have a lower specific modulus compared to insect cuticle values given in Wainwright *et al.*, by having a lower modulus with about the same density (E/p = 5.1–7.9 for 2 insects, and 1.0–2.3 for *A. fiordensis* and *A. salix*, respectively). If the Young's modulus given for *Cirripathes* sp. ($E = 0.3$ GN m^{-2}) in Wainwright *et al.* (1976) is combined with our density measurement of 1.1 in *C. luetkeni* Brook from the Bahamas (see Goldberg, 1976 for description), a skeleton of even lower specific modulus results (E/p = 0.27). The Young's moduli of the two *Antipathes* species differ by more than twofold, but range from 4.1 to 10.7 times stiffer than that reported for *Cirripathes* sp. by Wainwright *et al.* (1976). Antipatharians of this genus, unlike the ones we studied, are unbranched and whip-

Table I

Material properties of antipatharian skeletons

Properties	*Antipathes fiordensis*	*Antipathes salix*	Test statistics
I) Young's Modulus (GN/m^2)	1.24 (0.360); n = 31	3.20 (0.511); n = 23	$\chi^2 = 38.89$; $P < 0.0001$
II) Extensibility (mm/cm)	7.37 (1.667); n = 31	3.84 (0.783); n = 23	$\chi^2 = 36.95$; $P < 0.0001$
III) Density (g/cm^3)	1.25 (0.096); n = 15	1.40 (0.058); n = 25	$\chi^2 = 19.45$; $P < 0.0001$
IV) Hardness (Mohs)	3	3	
V) Microhardness (HV)			
i) Long Axis	18.2 (1.473); n = 3	22.1 (0.378); n = 3	$\chi^2 = 3.857$; $P < 0.05$
ii) Short Axis	20.3 (3.342); n = 3	22.8 (0.987); n = 3	$\chi^2 = 0.429$; $P > 0.05$

Means and standard deviations (in parentheses) are provided along with numbers of observations (n). The Kruskal-Wallis One-Way ANOVA by ranks (Chi-squares corrected for ties) were calculated to note differences between the two species.

Table II

Chemical composition of antipatharian skeletal tips

Properties	*Antipathes fiordensis*	*Antipathes salix*	Test statistics
I) Water content (% dry wt.)	21.1 (0.59); n = 15	19.6 (0.72); n = 25	$\chi^2 = 20.63$; $P < 0.0001$
II) Chitin content (% org. wt.)	10.4 (2.20); n = 8	14.7 (1.25); n = 3	$\chi^2 = 5.04$; $P < 0.05$
III) Protein content (% org. wt.)	55.4 (2.93); n = 8	51.3 (0.58); n = 3	$\chi^2 = 6.00$; $P < 0.025$
IV) Lipid content (% dry wt.)	0.32 (0.70); n = 25	0.22 (0.503); n = 25	$\chi^2 = 0.32$; $P > 0.05$

Means are followed by standard deviations (in parentheses) along with numbers of observations (n). Kruskal-Wallis One-Way ANOVA by ranks (Chi-squares corrected for ties) were calculated to note differences between the two species.

like, often forming corkscrew-like shapes on cliff faces of the reef. The low Young's modulus may structurally reflect this idiosyncrasy. Unfortunately, the correlative architectural properties of this genus are unknown.

Mechanical properties of gorgonian skeleton have been reported (Goldberg *et al.*, 1984; Jeyasuria and Lewis, 1987; Esford and Lewis, 1990), and although the two systems differ structurally and chemically (collagen instead of chitin, and distinct amino acid composition among other differences) the Young's moduli of the two black corals fall within the range (1.1–9.3 GN m^{-2}) reported for the tips of 13 gorgonians by Esford and Lewis (1990). Interestingly, they found that stiffer axes were typical of species from deeper water but unlike antipatharians, gorgonian skeletons from such environments are often calcified.

Table III

Organic composition of skeletal powder after formic acid and sodium borohydride treatment compared to untreated materials

	Antipathes fiordensis	*Antipathes salix*
Amino acids		
ASP	−6.8 (*)	5.9 (**)
THR	−9.6	0.8
SER	−2.4 (ns)	6.2 (*)
GLU	6.8	10.7
PRO	−14.7	9.5
GLY	2.6 (ns)	5.3 (*)
VAL	−13.7	−18.4
MET	−40.0	−10.0
ILE	−18.6	−11.7
LEU	0.1	4.3
TYR	−13.5 (ns)	−17.3 (*)
PHE	−39.1 (**)	−14.5 (ns)
HIS	8.1 (**)	7.6 (*)
TRP	−100.0 (**)	−100.0 (*)
LYS	−56.2	−48.2
ARG	−10.6	0.1
Protein	−6.1 (ns)	−8.7 (*)
Chitin	8.4 (ns)	13.7 (*)

(ns) not significant; (*) $P < 0.05$; (**) $P < 0.025$.

Changes are noted as percent decreases (negative values) or increases (positive values) from organic composition of untreated skeleton. All values are means of three trials and statistical differences were analyzed as in previous tables.

There is a growing body of evidence showing a relationship between skeletal mechanics and ecological function. In organisms with flexible skeletons, orientation to flow can maximize efficiency of suspension feeding and minimize drag forces (reviewed by Wainwright *et al.*, 1976). In certain gorgonian corals, adaptation to flow may be recorded in the skeleton as a change in preferred orientation of fan-like species (Wainwright and Dillon, 1969; Grigg, 1972; Velimirov, 1976). In branched gorgonians the skeleton can be reinforced perpendicular to the direction of flow, by deposition of carbonate (Wainwright and Koehl, 1976; Wainwright *et al.*, 1976). Preferred orientation occurs in the Antipatharia (Warner, 1981), and there is a degree of it exhibited in *A. fiordensis*. Colonies near the mouths of the fiords, are subjected to more consistent current fields, resulting in more fan-shaped colonies. Otherwise, this species tends to branch in multiple planes (Grange, 1988). In addition, the skeleton is often elliptical in cross section, especially in the thicker branches, with the compressed sides facing the predominant current flow. In *A. salix*, there is no obvious structural asymmetry, and the colonies tend to be branched in many planes. Antipatharians generally require low rheological environments. Unlike other cnidarians, the polyps have no structural protection from the abrasive forces associated with strong current. The muscular systems of the polyps and tentacles are so poorly developed that a modest contraction is their only apparent defense against such forces (Goldberg and Taylor, 1989). Transplant experiments into relatively shallow water further suggest that abrasion is a major source of mortality (Grigg, 1965). Thus the substantial structural and mechanical properties of the black coral skeleton seem to be overdesigned for the deeper and hydrodynamically more docile zones in which antipatharians are generally found. It

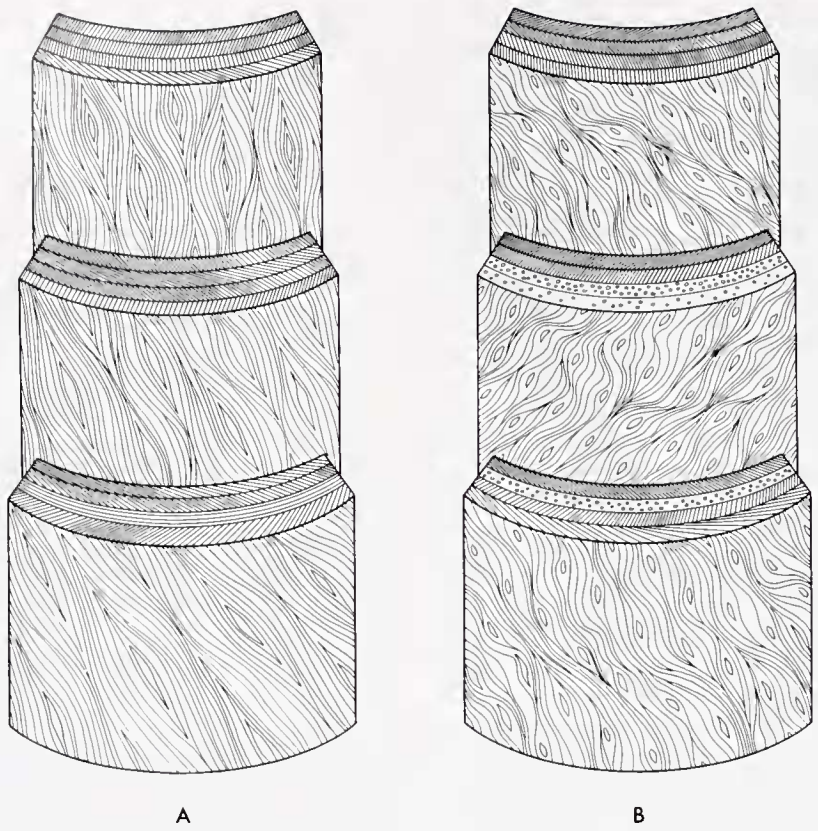

Figure 22. Composite sketch of fibril patterns. (A) *Antipathes salix* is shown with surface fibrils helically wound in an anticlockwise direction. The gradual change in the rotational sense of the winding pattern is shown in successive longitudinal sections. Spines are shown as the centers of the fibrillar pattern. Transverse sections through adjacent layers depict gradual, angular changes in fibril orientation as well as layers with little or no change. (B) *Antipathes fiordensis* is depicted with a swirling pattern of fibrils that generally tend anticlockwise. The more numerous spines are shown as focal points for the surface fibril pattern. Abrupt layer-to-layer changes in fibril orientation are characteristic of this species. No two adjacent layers have the same fibril pattern.

seems counterintuitive to find such stiff skeletons in zones of relatively low velocity water movement.

While the fit between ecological function and skeletal design is unclear, the distinction between the two species studied has shown that *Antipathes salix* is darker, harder, more dense, more hydrophobic, and stiffer than *A. fiordensis*. These material differences appear to reflect the more considerable commercial value of *A. salix* in the jewelry trade.

Acknowledgments

We thank W. Faulkner of Telectronics Pacemakers Corp. for his assistance with microhardness testing and R. Nutt for the illustrations. Both K. Gordon (Biology) and C. Levy (Mechanical Engineering) at FIU contributed substantially to the mechanical analysis. We also thank K. Gordon, K. Grange, and two anonymous reviewers for helpful comments on the manuscript. This work was supported by NSF grant OCE-8613884 (to W.G.). New Zealand coral material was obtained with the assistance of K. Grange and R. Singleton of DSIR, Wellington, and the support of the U.S.-New Zealand Cooperative Science Program, as well as funds from DSIR. The Florida Institute of Oceanography provided ship time and facilities to support the collection of Bahamian coral material. Collecting permits from the Governments of New Zealand and the Bahamas are also gratefully acknowledged.

Literature Cited

Bassin, M., G. M. Brodsky, and H. Wolkoff. 1979. *Statics and the Strength of Materials,* 3rd Ed. McGraw-Hill, Toronto.

Barth, F. G. 1973. Microfiber reinforcement of an arthropod cuticle. Laminated composite material in biology. *Z. Zellforsch.* **144:** 409–433.

Bouligand, Y. 1965. Sur une architecture torsadée répandue dans les nombreuses cuticles d'arthropodes. *C.R. hebd. Seances Acad. Sci. Paris* **261:** 3665–3668.

Bouligand, Y. 1971. Les orientations fibrillaires dans le squelette des Arthropods 1. L'example des crabes, l'arrangement torsadé des strates. *J. Microsc. (Paris)* **11:** 441–472.

Bouligand, Y. 1972. Twisted fibrous arrangements in biological materials and cholesteric metaphases. *Tissue & Cell* **4:** 189–217.

Compere, P., and G. Goffinet. 1987. Aspects ultrastructureaux et fonctionnels de diverses régions cuticulaires non minéralisées d'un crustacé décapode, *Carcinus maenas*. *Ann. Soc. R. Zool. Belg.* **117:** 159–173.

Dalingwater, J. E. 1975. The reality of arthropod cuticular laminae. *Cell Tissue Res.* **163:** 411–413.

Dennell, R. 1973. The structure of the cuticle of the shore crab, *Carcinus maenas*. *Zool. J. Linn. Soc.* **52:** 159–163.

Esford, L. E., and J. C. Lewis. 1990. Stiffness of Caribbean gorgonians (Coelenterata, Octocorallia) and Ca/Mg content of their axes. *Mar. Ecol. Prog. Ser.* **67:** 189–200.

Filshie, B. K. 1982. Fine structure of the cuticle of insects and other arthropods. Pp. 281–312 in *Insect Ultrastructure,* Vol. 1, R. King and H. Akai, eds. Plenum Press, New York.

Giraud-Guille, M. M. 1984. Fine structure of the chitin-protein system in the crab cuticle. *Tissue & Cell* **16:** 75–92.

Goldberg, W. M. 1976. A comparative study of the chemistry and structure of gorgonian and antipatharian coral skeletons. *Mar. Biol.* **35:** 253–267.

Goldberg, W. M. 1978. Chemical changes accompanying maturation of the connective tissue skeletons of gorgonian and antipatharian corals. *Mar. Biol.* **49:** 203–210.

Goldberg, W. M. 1991. Chemistry and structure of skeletal growth rings in the black coral *Antipathes fiordensis* (Cnidaria, Antipatharia). *Hydrobiologia* **216:** 403–409.

Goldberg, W. M., J. Makemson, and S. B. Colley. 1984. *Entocladia endozoica* sp. nov., a pathogenic chlorophyte: structure, life history, physiology and effect on its coral host. *Biol. Bull.* **166:** 368–383.

Goldberg, W. M., and G. T. Taylor. 1989. Cellular structure and ultrastructure of the black coral *Antipathes aperta*: 1. Organization of the tentacular epidermis and nervous system. *J. Morphol.* **202:** 239–253.

Grange, K. R. 1985. Distribution, standing crop, population structure and growth rates of black coral in the southern fiords of New Zealand. *NZ J. Mar. Freshw. Res.* **19:** 467–475.

Grange, K. R. 1988. Redescription of *Antipathes aperta*. Totton, (Coelenterata: Antipatharia), an ecological dominant in the southern fiords of New Zealand. *NZ J. Zool.* **15:** 55–61.

Grange, K. R. 1990. *Antipathes fiordensis*, a new species of black coral (Coelenterata: Antipatharia) from New Zealand. *NZ J. Zool.* **17:** 279–282.

Grigg, R. 1965. Ecological studies of black coral in Hawaii. *Pac. Sci.* **19:** 244–260.

Grigg, R. W. 1972. Orientation and growth in sea fans. *Limnol. Oceanogr.* **17:** 185–192.

Gubb, D. 1975. A direct visualization of helicoidal architecture in *Carcinas maenas* and *Halocynthia papillosa* by scanning electron microscopy. *Tissue & Cell* **7:** 19–32.

Hackman, R. H., and M. Goldberg. 1971. Studies on the hardening and darkening of insect cuticles. *J. Insect Physiol.* **17:** 335–347.

Hepburn, H. R., and H. D. Chandler. 1976. Material properties of arthropod cuticles: the arthrodial membranes. *J. Comp. Physiol.* **109:** 177–198.

Hepburn, H. R., and H. D. Chandler. 1980. Materials testing of arthropod cuticle preparations. Pp. 1–44. in *Cuticle Techniques in Arthropods*, T. A. Miller, ed. Springer-Verlag, New York.

Hepburn, H. R., and I. Joffe. 1976. On the material properties of insect exoskeletons. Pp. 209–235 in *The Insect Integument*, H. R. Hepburn, ed., Elsevier, New York.

Hickson, S. J. 1924. *An Introduction to the Study of Recent Corals.* Manchester University Press, Longmans, Green & Co., London. 257 p.

Hillerton, J. E. 1984. Cuticle: mechanical properties. Pp. 626–637 in *Biology of the Integument 1. Invertebrates*, J. Bereiter-Hahn, A. G. Matolsky, and K. S. Richards, eds. Springer-Verlag, New York.

Hillerton, J. E., S. E. Reynolds, and J. F. V. Vincent. 1982. On the indentation hardness of insect cuticle. *J. Exp. Biol.* **96:** 45–52.

Holl, S. M., J. Schaefer, W. M. Goldberg, K. J. Kramer, T. D. Morgan, and T. L. Hopkins. 1992. Comparison of black coral skeleton and insect cuticle by a combination of carbon-13 NMR and chemical analyses. *Arch. Biochem. Biophys.* **292:** 107–111.

Hughes, P. M. 1987. Insect cuticular growth layers seen under the scanning electron microscope: a new display method. *Tissue & Cell.* **19:** 705–712.

Hunt, S., and K. Oates. 1984. Chitin helicoids accompany protein helicoids in the periostracum of a whelk, *Buccinum. Tissue & Cell* **16:** 565–575.

Jeyasuria, P., and J. C. Lewis. 1987. Mechanical properties of the axial skeletons on gorgonians. *Coral Reefs* **5:** 213–219.

Neville, A. C. 1967. Chitin orientation in cuticle and its control. *Adv. Insect Physiol.* **4:** 213–286.

Neville, A. C. 1970. Cuticle ultrastructure in relation to the whole insect. *Symp. R. Entomol. Soc. Lond.* **5:** 17–39.

Neville, A. C. 1984. Cuticle: organization. Pp. 611–625 in *Biology of the Integument 1. Invertebrates*, J. Bereiter-Hahn, A. G. Matolsky, and K. S. Richards, eds. Springer-Verlag, New York.

Neville, A. C., and B. M. Luke. 1969. A two-system model for chitin-protein complexes in insect cuticles. *Tissue & Cell* **1:** 689–707.

Opresko, D. M. 1972. Redescription and reevaluations of the antipatharians described by L. F. De Pourtales. *Bull. Mar. Sci.* **22:** 950–1017.

Simpson, R. J., M. R., Neuberger, and T. Y. Liu. 1976. Complete amino analysis of protein from a single hydrolysate. *J. Biol. Chem.* **251:** 1936–1940.

Velimirov, B. 1976. Variation in growth form of *Eunicea cavolinii* Koch (Octocorallia) related to water movement. *J. Exp. Mar. Biol. Ecol.* **21:** 109–117.

Vincent, J. F. V. 1980. Insect cuticle: a paradigm for natural composites. *Symp. Soc. Exp. Biol.* **34:** 183–210.

Vincent, J. F. V., and J. E. Hillerton. 1979. The tanning of insect cuticle—a critical review and a revised mechanism. *J. Insect Physiol.* **25:** 653–658.

Wainwright, S. A., and J. R. Dillon. 1969. On the orientation of sea fans (genus *Gorgonia*). *Biol. Bull.* **136:** 130–139.

Wainwright, S. A., and M. A. R. Koehl. 1976. The nature of flow and the reaction of benthic Cnidaria to it. Pp. 5–21 in *Coelenterate Ecology and Behavior*, G. O. Mackie, ed. Plenum Press, New York.

Wainwright, S. A., W. D. Biggs, J. D. Currey, and J. M. Gosline. 1976. *Mechanical Design in Organisms.* Edward Arnold Publ. Ltd., London. 423 pp.

Warner, G. F. 1981. Species descriptions and ecological observations of black corals (Antipatharia) from Trinidad. *Bull. Mar. Sci.* **31:** 147–163.

Wood, E. M., and S. M. Wells, 1988. The Marine Curio Trade: Conservation Issues. A report for the Marine Conservation Society, Herefordshire, England. Pp. 1–120.